Metal Nanoparticles Based Inkjet Ink for Advanced Circuit Board Application

Osama A. Fouad[1,*], Fatma Morsy[2], Samya El-Sherbiny[2,*] and Diaa Abd Elshafy[2]

[1]*Central Metallurgical Research and Development Institute, CMRDI, P.O. Box: 87 Helwan 11421, Cairo, Egypt*

[2]*Paper and Printing Lab., Chemistry Department, Faculty of Science, Helwan University, Helwan, Egypt*

Abstract: This study investigates the synthesis of mono metallic (copper and silver) and bi-metallic (copper/silver core/shell) conductive nanopigments for inkjet printing. Polyethylene glycol (PEG) was used as a main reducing agent followed by polyvinylpyrrolidone (PVP) as a capping and dispersing agent. From the XRD, TEM, and SEM analyses, the synthesized mono and bi metallic particles were confirmed to be in a nano scale with particle size 7, 8.5 and 15.5 nm for copper, silver and copper/silver core/shell, respectively. The prepared nanopigments were included in inkjet ink formulation and printed on flexible polyethylene terephthalate (PET) films. The printed ink films were sintered at various temperatures (110, 150, 200). The results revealed that the resistivity of these particles was reduced by sintering and the resistivity of Cu, Ag and Cu/Ag patterns sintered in air at 200 ºC for 30 min were 3.1, 2.99 and 4.14 µΩ-cm, respectively. The obtained results were in a good agreement with the published ones and insured the promising using of our products in metal-based inkjet printed circuit boards (PCB).

Keywords: Metal nanoparticles, silver, copper, Cu/Ag core/shell, conductive ink, printed circuit.

1. INTRODUCTION

Printed electronics by means of inkjet printing have received great attention in recent years [1]. Inkjet-printed electronics have many advantages in reducing consumption of raw materials, eco-friendly, simplicity and high productivity process over the conventional printing processes [2]. It has opened a new world of low-cost printed circuit boards based on conductive metal nanoparticles aiming at high-volume electronic market areas [3]. The printing of conductive patterns on flexible substrates has been achieved for various applications, including flexible electronic displays [4], flexible antennas [1], solar cells [5] and sensor for diagnosis using various conductive nanopigments such as carbon, silver and copper.

Silver nanoparticles have been used in different applications such as catalysis, optics, and surface-enhanced Raman scattering [6]. Noble metals such as gold and silver have mainly been utilized in printing highly conductive elements in electronic devices [7]. Moreover, the printing of metal inks, especially those containing silver nanoparticles, has been found to be a very powerful tool for direct patterning of electrically conductive interconnects in electronic devices [8]. The high price of silver nanoparticles despite their high conductivity and the increasing demands of reducing production cost led to find alternative nanopigment in conductive ink [9]. Copper as a cheap and conductive material was found more favorable for this approach [7]. Its advantages lie in that Cu nanoparticles are cheap, have high yields under mild reaction conditions and have short reaction time [9]. Nanocopper inks have been used for printing of flexible conductive surfaces in diodes, transistors, low-cost sensors, electrical circuits and radio frequency identification tags (RFID tags) [10].

Cu nanoparticles have been synthesized through different methods such as thermal decomposition [11], metal salt reduction [12], microwave heating [13], radiation methods [14], microemulsion techniques [15]. Cu nanoparticles can easily oxidize to form copper oxide. To avoid oxidation, the reduction methods are usually performed under an inert atmosphere (argon, nitrogen) [16], inorganic solvents [17] or microemulsion systems [18] and in presence of protective polymers [19] or surfactants [20]. Bimetallic or multi-metallic nanoparticles can be synthesized by the co-reduction of two or more kinds of metal ions forming nanoalloys. Reductive deposition of one kind of metal ion over another reduced metal nucleus results in forming core/shell nanoparticles [21].

In this work, is reported the synthesis of a stable Cu and Ag nanoparticles and nano Cu/Ag core/shell particles combining the properties of both copper and silver using a simple method. The prepared nanoparticles were used as pigments in inkjet conductive ink formulation. These inks were printed on

*Address correspondence to these authors at the Central Metallurgical Research and Development Institute, CMRDI, P.O. Box: 87 Helwan 11421, Cairo, Egypt; Tel: +202-25010642; Fax: +202-25010639;
E-mail: oafouad@yahoo.com

Paper and Printing Lab., Chemistry Department, Faculty of Science, Helwan University, Helwan, Egypt; Tel/Fax: +202-25552468;
E-mail: samya.elsherbiny@gmail.com

E-ISSN: 2311-8792/17

flexible PET films and sintered at various temperatures to obtain the optimum conductivity (lower resistivity) with good performance. The preparation of bimetallic aimed at reducing production cost of the ink upon using copper nanoparticles and to protect the copper nanoparticles from oxidation using silver as a shell.

2. EXPERIMENTAL

2.1. Materials

Silver Nitrate ($AgNO_3$. 99 %, Sigma-Aldrich) and Copper Acetate Trihydrate ($Cu(CH_3COO)_2.3H_2O$, 95 %, El-Nasr) were used as a silver and copper precursor, respectively. Polyethylene glycol (PEG, Mw=6000, Carl Roth) was used as a reducing agent. Polyvinylpyrrolidone (PVP Mw= 40000, Sigma-Aldrich) was selected as a protective polymer and dispersing agent. Ethanol (C_2H_5OH, 95 %, El-Nasr) was used as a solvent in preparation of metallic nanoparticles. For ink formulation; vinyl chloride/vinyl acetate copolymers (Binder) and Cyclohexanone and Ethylene glycol ethers (Cellosolve) were chosen.

2.2. Preparation of Mono Metallic Copper and Silver Nanoparticles

For preparation of mono metallic copper and silver nanoparticles, initial trials were done using different concentrations of copper acetate and silver nitrate. Solutions of 0.1, 0.01 and 0.001 mMol were prepared. It was found that 0.01 mMol was the suitable concentration of both copper and silver ion salts. Their higher concentration (0.1 mMol) caused agglomeration of the prepared nanoparticles, while the very diluted concentration (0.001 mMol) yielded low percent of the nanoparticles. In addition, the effect of pH on the stability of the prepared nanoparticles was studied at various pH values. Acidic and alkaline solutions caused precipitation of the metal. The suitable pH of the media was found to be nearly neutral (pH = 7.4).

For a typical preparation of Cu or Ag nanoparticles in ambient atmosphere, 0.01 mMol of copper acetate trihydrate [$Cu(CH_3COO)_2.3H_2O$] or silver nitrate [$AgNO_3$] were added to 50 ml (0.01 mMol) polyethylene glycol and 50 ml (0.01 mMol) polyvinylpyrrolidone in a single-neck round-bottom flask. Then the mixture was magnetically stirred with 10 ml ethanol until complete dissolution of copper or silver salts. The mixture solutions were then heated to 80 ºC for about 2 hours. At the end of the reaction time, the solutions were left to cool down to room temperature (solution A for Cu and solution B for Ag). The suspended particles were separated by centrifugation and were washed with ethanol for several times before vacuum drying at 40 ºC for1 hour and packing for further testing.

2.3. Preparation of bi Metallic Copper/Silver (Core/Shell) Nanoparticles

The synthesis of bi metallic core/shell nanoparticles, has been done in two main steps:

1. Synthesis of mono metallic nanoparticles (M_1) which in this case is core.

2. Synthesis of bimetallic nanoparticles by adding the second metal ion salt ($M_2^{+}{}_{(aq)}$) to the first metal salt solution one.

Figure **1** shows the schematic preparation of M_1/M_2 core/shell [22].

Preparation of Cu/Ag Core/Shell Nanoparticles

Copper nanoparticles (solution A) was prepared (as mentioned before) and then heated for 15 min at 80 °C. 25 ml (0.01 mMol) of silver nitrate were added to the solution during stirring at a constant rate and heated for another 3 hours; a grayish black colloidal solution was formed (solution C). The resulting particles were separated by centrifugation and washed with ethanol. Afterwards they were exposed to vacuum drying at 40 ºC for one hour and packed for further testing.

The prepared Cu, Ag and Cu-Ag nanoparticles are shown in Figure **2**.

2.4. Formulation of Inkjet Conductive Ink

For inkjet ink preparation, the nano pigments (Cu, Ag and Cu/Ag) were separately dispersed in the binder mixture of vinyl chloride/vinyl acetate copolymer by stirring at constant rate for one hour, and then the solvents cyclohexanone and ethylene glycol ethers (Cellosolve) were added and stirred for 15 min. Table **1** shows the formulation of inkjet conductive ink [23].

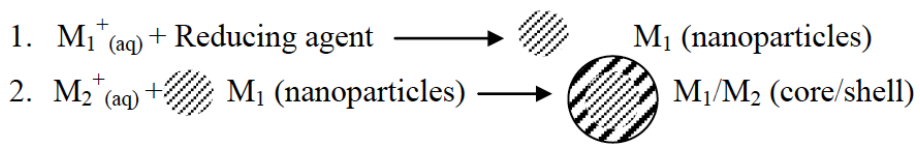

Figure 1: Schematic representation preparation of M_1/M_2 core/shell.

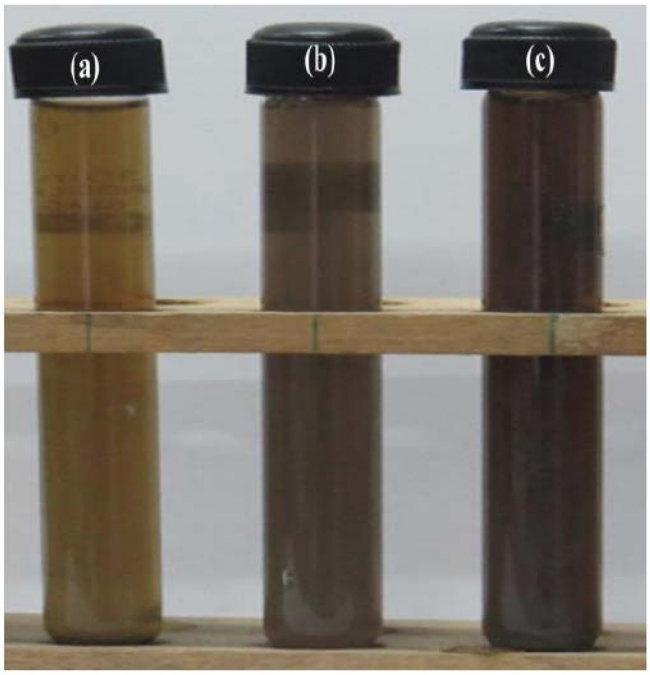

Figure 2: As prepared (**a**) Cu, (**b**) Cu-Ag and (**c**) Ag nanoparticles.

Table 1: Conductive Ink Formulation

Constituents	Percent (wt/wt %)
Pigments (Metallic nanoparticles)	33.33
Binder (vinyl chloride/vinyl acetate copolymer)	6.67
Solvent (cyclohexanone and ethylene glycol ethers (Cellosolve))	60
Total	100 %

2.5. Printing of Inkjet Conductive Inks on PET Films

The formulated inks were printed on flexible Polyethylene Terephthalate (PET) films using hp Deskjet d1600 printer. Many trials were done to obtain uniform and smooth film thickness of printed inks. The patterned films were dried at 65 °C, and subsequently sintered at various temperatures 110, 150 and 200 °C to obtain good patterns with the lowest possible resistivity.

2.6. Materials Characterization

The purity, formed phases and crystallite sizes of Cu, Ag and Cu/Ag core/shell nanoparticles were investigated by X-ray powder diffraction (XRD, D/Max 2500 PC, Rigaku, Japan) using Cu target operating on 40 kV and 100 mA (with a scan speed of 4°/min) with Cu-Kα radiation of wavelength equals 1.54059 Å. The θ -2θ scan was done in the range 0°–80°. The morphology and size distribution of the particles before and after sintering were characterized by transmission electron microscope (TEM, JEM-2100, Japan) operated at 200 kV. Samples for TEM investigation were prepared by placing a drop of colloidal dispersion on the carbon-coated copper grid and then allowing the drops to dry in air. Surface scan was performed using scanning electron microscope (SEM, S-4800, Hitachi, Japan) at a voltage of 2.0 kV. Gloss is a property that refers to the quality of luster, or ability of the surface to show an image. A micro glossmeter was used, at an angle of 75 to measure the gloss of printed films.

The resistivity of the printed patterns was measured by a 4-point probe (QuadPro-301, Russia). The thermal characteristic of the printed copper, silver and copper-silver core/shell inks were analyzed with a thermal gravity analyzer (TGA: STA 499C, NETZSCH); it was measured in the temperature range of 280–800 °C, at a rate of 10 °C/min and in 3% H_2 atmosphere.

3. RESULTS AND DISCUSSION

3.1. Characterization of Mono Metallic Nanoparticles

The XRD patterns of the prepared copper and silver nanoparticles are shown in Figure **3**. Three characteristic peaks for metallic copper (Cu, JCPDS card #(04-001-3178)) are observed at 2θ = 43.2°, 50.6°, 74.1°, respectively, Figure **3a**. The peaks belong to XRD planes (111), (200) and (220), respectively. On the other hand, four main characteristic peaks at 2θ = 38.1º, 44.29º, 64.5º, 77.45º are observed in Figure **3b**. These peaks belong to XRD planes of metallic silver (Ag, JCPDS card # 03-065-2871) (111), (200), (220) and (311), respectively. The crystallite size could be calculated for the prepared nanoparticles using Debye-Scherrer's formula, as follows:

$$\tau = k \lambda / \beta \cos \theta$$

Where τ is the mean of the crystallite size, k = 0.9 is a correction factor accounts for particle shapes, λ is the wavelength of Cu target (Kα radiation), β is the full width at half maximum (FWHM) of the most intense diffraction peak, θ is the Braggs diffraction angle. The average crystallite sizes of copper and silver nanoparticles are around 6 and 8.8 nm, respectively.

TEM images in Figure **4a,b** shows that agglomerated copper nanoparticles have a quasi-spherical shape with average particle size up to 7 nm.

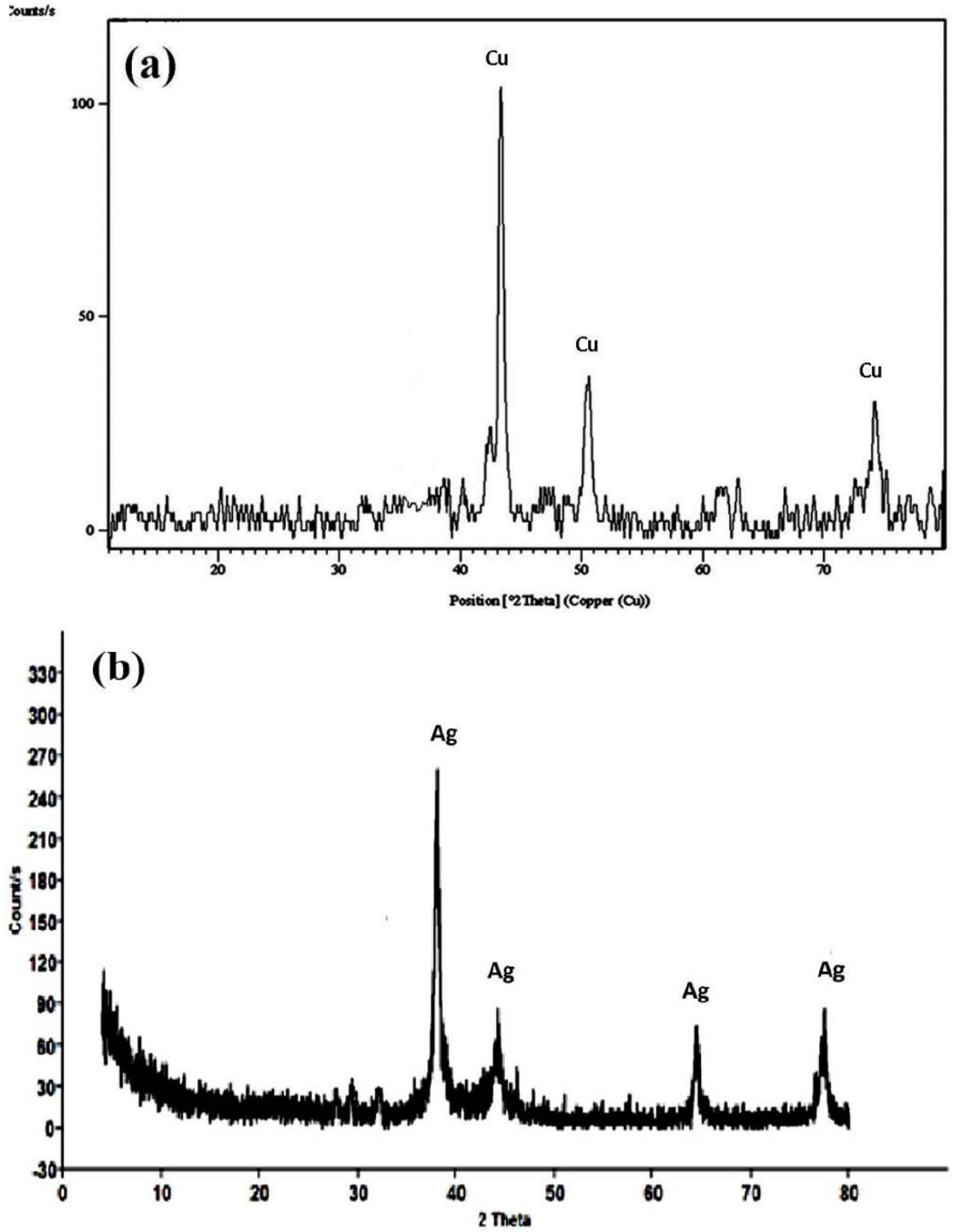

Figure 3: XRD pattern of (a) copper nanoparticles (b) silver nanoparticles.

Whereas Figure **4c,d** shows that silver nanoparticles have well defined spherical shape with average particle size up to 8.5 nm. The protective shell in Figure **4b** is due to capping agent PVP [24]. The high dispersivity of silver nanoparticles indicates that they are much more stable than copper nanoparticles. The particle size distribution of the prepared copper and silver nanoparticles that were obtained from TEM images confirmed that the prepared materials were formed in nano scale. These results are in agreement with that obtained XRD results.

3.2. Characterization of bi Metallic and Core/Shell Nanoparticles

Figure **5** shows two main characteristic peaks at 2θ = 38.4º, 44.6º which indicate the presence of copper/silver (core/shell). From Scherrer's formula, the average crystallite size of copper/silver nanoparticles was about 8 nm.

Figure **6a-b** shows the TEM images of the synthesized copper/silver bi metallic nanoparticles. The figure shows the presence of core/shell. This result is in

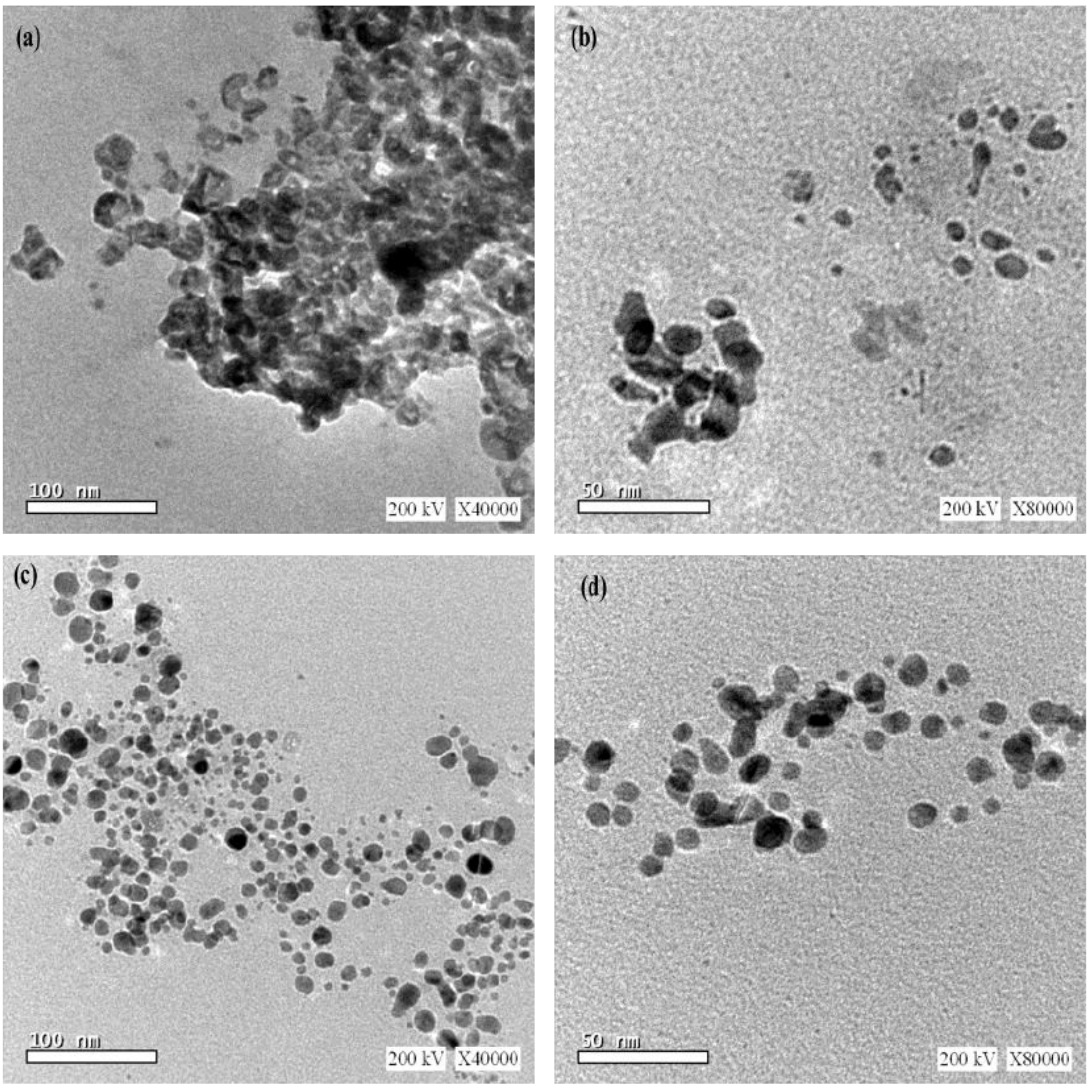

Figure 4: TEM images of (**a**,**b**) synthesized copper nanoparticles and (**c**,**d**) synthesized silver nanoparticles.

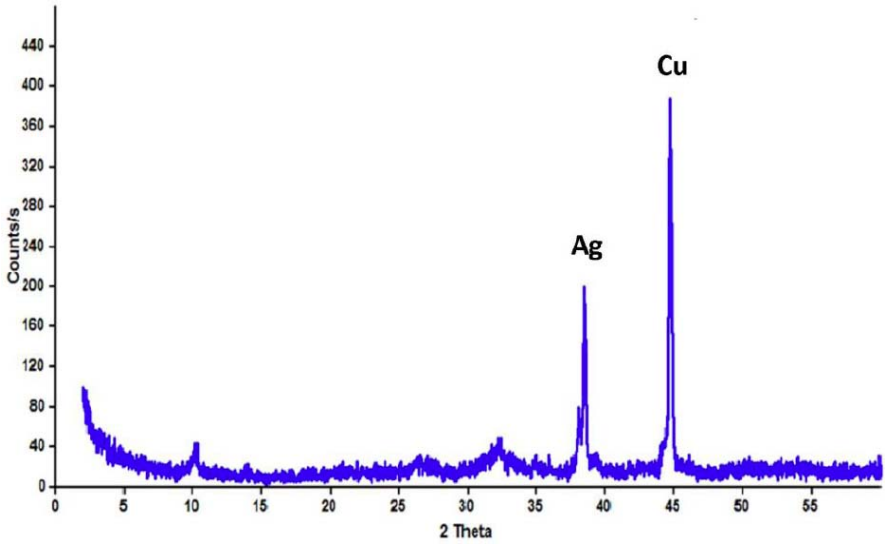

Figure 5: XRD pattern of copper/silver (core/shell) nanoparticles.

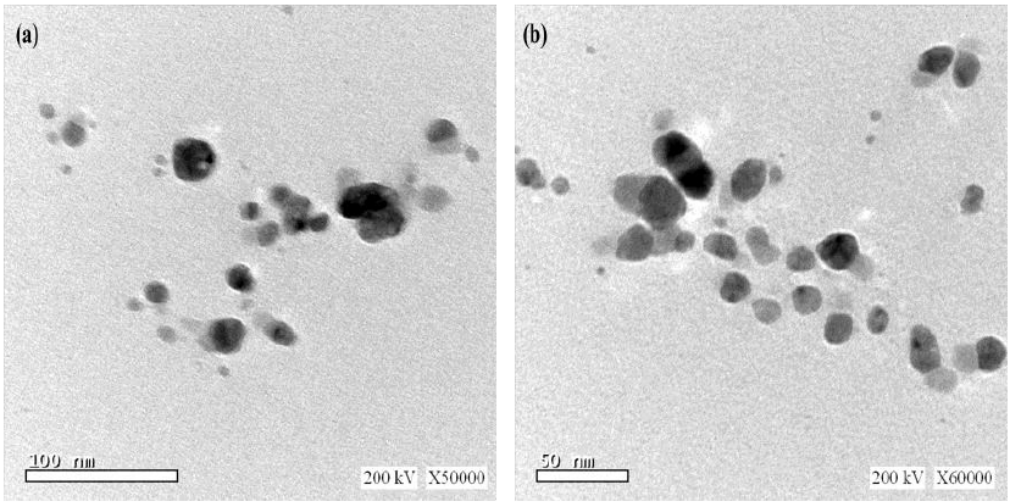

Figure 6: TEM images of (**a**, **b**) synthesized copper/silver bi metallic (core/shell) nanoparticles.

agreement with the obtained data from XRD results (Figure **5**). TEM images show that the particle size of the prepared copper/silver nanoparticles was found to be in nano scale (about 15.5 nm).

4. CHARACTERIZATION OF CONDUCTIVE INKJET PRINTED FILMS

4.1. SEM Analysis

SEM images of copper, silver and copper/silver nanoparticles printed samples sintered at 110 and 200 ºC for 30 min are shown in Figure **7a-e**. The sintered Cu and Ag nanoparticles printed films at 110 ºC appear as agglomerated needles as shown in Figure **7a** and **7c**, respectively. The degree of agglomeration increased at 200 ºC for both Cu and Ag nanoparticles printed sintered films, as shown in Figure **7b** and **7d**, respectively. The particles form continuous and well distributed films, which consistent is with the decrease in resistivity with increased temperature Table **2**). In Figure **7e**, the particles of copper/silver (core/shell) sintered at 200 ºC show lack of continuous film rather agglomerated particles leading to increasing the resistivity.

4.2. Films' Resistivity Measurements

Table **2** illustrates the results of films' resistivity measurements of each printed patterns at various sintering temperatures 110, 150 and 200 ºC. The results show that the resistivity of all films decreased as the sintering temperature increased. This may be due to particles agglomeration and/or coalescence. Silver nanoparticle based ink printed films had the lowest resistivity at all sintering temperatures. The lowest obtained resistivity of ink patterns of copper, silver and copper/silver nanoparticles sintered at 200 °C for 30 min were 3.1, 2.99 and 4.14 μΩ-cm, respectively compared with the bulk Cu wire resistivity which is 1.67 μΩ-cm. The difference may be due to film discontinuity and/or thin printed film. Lee *et al.* [9] reported 4.4 μΩ-cm film resistivity when they annealed printed copper samples at 320 ºC for 20 min which is higher than the one obtained in our work. The reported values for copper and silver printed samples at various temperatures were also found to be higher than our obtained results [2, 25-29].

4.3. Gloss Measurements

Figure **8** shows the gloss percentage of the printed films at different sintering temperatures. The figure shows that as the sintering temperature increased the gloss of the printed samples increased. This might be due to particles' agglomeration or coalescence forming continuous ink film. This caused increasing of the smoothness and consequently the gloss percentage of the printed films. Printed Ag nanopigment samples have higher gloss percentage than other printed samples; this may be due to the higher stability of silver nanoparticles which led to good dispersion.

4.4. Thermogravimetric Analysis (TGA)

Figure **9a-c** shows the thermogravimetric analysis (TGA) of all printed samples at different sintering temperatures. As shown in Figure **9a** the printed copper samples show good thermal stability up to 380 ºC, and then start to decompose and end at about 480 ºC. Also the sintering temperature of the printed copper samples affects their thermal stability as shown in Figure **9a**, the greater thermal stability was found to be at 200 ºC close to that of PET films. Figure **9b**

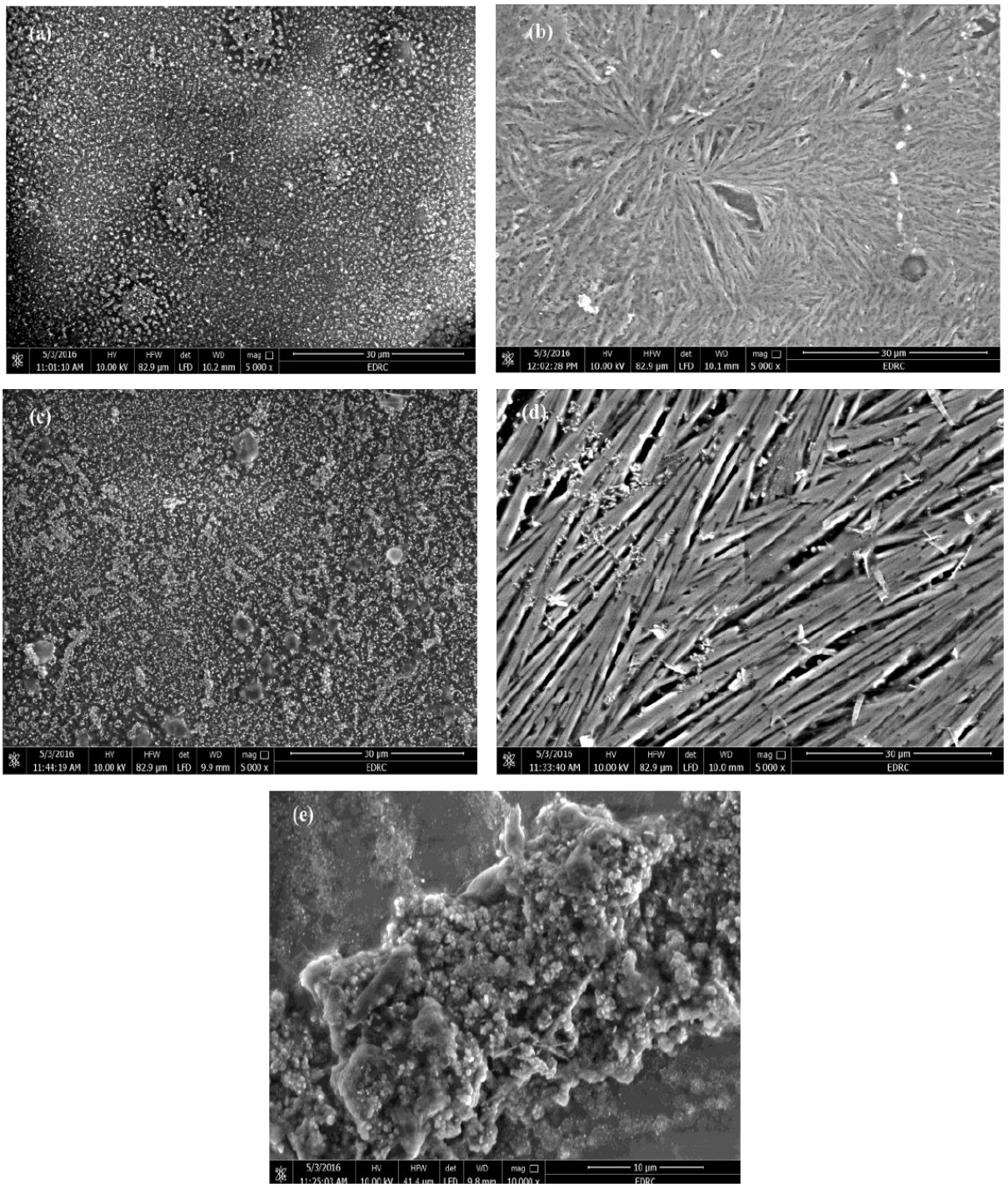

Figure 7: SEM of the printed samples with different nanoparticles and sintered at different temperatures (**a**) copper at 110 ºC (**b**) copper at 200 ºC (**c**) silver at 110 ºC (**d**) silver at 200 ºC (**e**) copper-silver at 200 ºC.

Table 2: Film Resistivity Results of Printed Samples

Sintering temperature	110 ºC	150 ºC	200 ºC
Cu	21.4μΩ-cm	11.3 μΩ-cm	3.1μΩ-cm
Ag	19.9 μΩ-cm	10.8 μΩ-cm	2.99 μΩ-cm
Cu/Ag	23.5 μΩ-cm	12.7 μΩ-cm	4.14 μΩ-cm

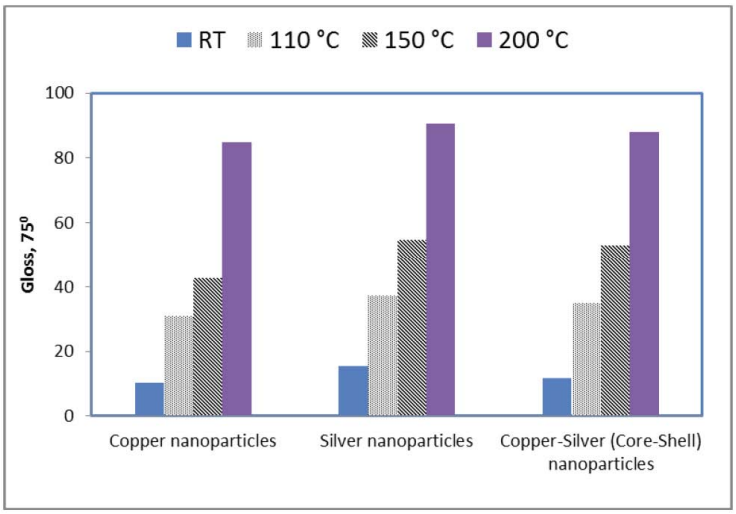

Figure 8: Gloss percentage of the printed films at room temperature (RT) and sintered films at 110, 150 and 200 ºC for 30 min.

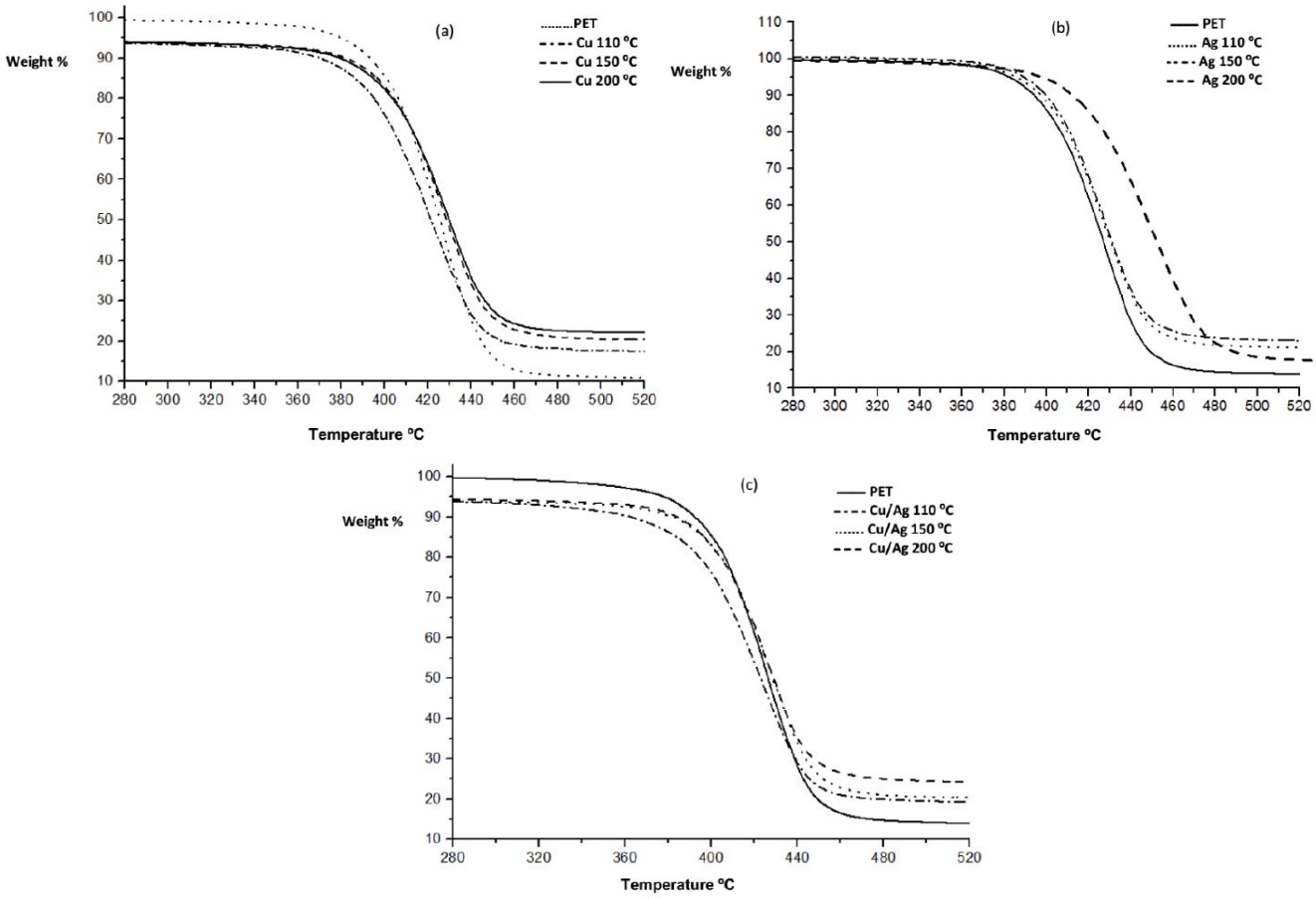

Figure 9: TGA of printed samples with the synthesized (**a**) copper (**b**) silver (**c**) copper/silver nanoparticles.

illustrates TGA of printed silver nanoparticles, which shows good thermal stability for all printed silver samples at different sintering temperatures. There exists a continuous weight loss at the temperatures ranging from 380-480 ºC, except for the printed silver samples which was sintered at 200 ºC. This shows great thermal stability up to 500 ºC, after which it was decomposed from 500-540 ºC. Figure **9c** shows the thermal stability of sintered printed copper/silver nanoparticles. It has lower thermal stability at 110 ºC sintering temperature. The stability increasing with increased sintering temperature TGA results for printed copper, silver and copper/silver samples are consistent with the results of resistivity measurements.

5. CONCLUSION

In this study mono metallic copper and silver nanoparticles and bi metallic copper/silver and silver/copper nanoparticles were prepared successfully from ionic liquids of the corresponding precursors. Several trials were done by using different concentrations of both copper and silver ion salts. The suitable concentration was found to be 0.01 mMol. pH affected the stability of the prepared nanoparticles, the suitable pH of the media being nearly neutral (pH = 7.4). The results of XRD and TEM confirmed that their crystallite and particle sizes were in nanoscale. The prepared nanoparicles were used as nanopigments for inkjet inks formulations. The lowest obtained resistivity for ink patterns of copper, silver and copper/silver nanoparticles sintered at 200 °C for 30 min were 3.1, 2.99 and 4.14 μΩ-cm, respectively which are lower than the recently reported work in literature. Silver nanoparticles show the lowest resistivity of ink patterns sintered at 200 ºC, its value was 2.99 μΩ-cm. These results were confirmed by studying the morphology and stability of nano pigment by SEM and TGA, respectively. The obtained results insured the promising use of the obtained products in metal-based inkjet printed circuit boards (PCB) at lower resistivity and lower sintering temperature.

REFERENCES

[1] Woo K, Kim D, Kim JS, Lim S, Moon J. Ink-jet printing of Cu-Ag-based highly conductive tracks on a transparent substrate. Langmuir 2009; *25*(1): 429-433. https://doi.org/10.1021/la802182y

[2] Cheon J, Lee J, Kim J. Inkjet printing using copper nanoparticles synthesized by electrolysis. Thin Solid Films 2012; 520(7): 2639-2643. https://doi.org/10.1016/j.tsf.2011.11.021

[3] Kosmala A, Zhang Q, Wright R, Kirby P. Development of high concentrated aqueous silver nanofluid and inkjet printing on ceramic substrates. Materials Chemistry and Physics 2012; 132 (2-3): 788-795. https://doi.org/10.1016/j.matchemphys.2011.12.013

[4] Chen Y, Au J, Kazlas P, Ritenour A, Gates H, McCreary M. Flexible active-matrix electronic ink display. Nature 2003; 423(6936): 136. https://doi.org/10.1038/423136a

[5] Otte K, Makhova L, Braun A, Konovalov I. Flexible Cu(In,Ga)Se2 thin-film solar cells for space application. Thin Solid Films 2006; (511-512)*:* 613-622. https://doi.org/10.1016/j.tsf.2005.11.068

[6] Nie S. Probing Single Molecules and Single Nanoparticles by Surface-Enhanced Raman Scattering. Science 1997; 275(5303): 1102-1106. https://doi.org/10.1126/science.275.5303.1102

[7] Jeong S, Woo K, Kim D, Lim S, Kim JS, Shin H, Moon J. Controlling the thickness of the surface oxide layer on Cu nanoparticles for the fabrication of conductive structures by ink-jet printing. Advanced Functional Materials 2008; 18(5): 679-686. https://doi.org/10.1002/adfm.200700902

[8] Faddoul R, Reverdy-Bruas N, Blayo A, Khelifi B. Inkjet printing of silver nano-suspensions on ceramic substrates - Sintering temperature effect on electrical properties. Microelectronic Engineering 2013; (105): 31-39. https://doi.org/10.1016/j.mee.2012.12.007

[9] Lee B, Kim Y, Yang S, Jeong I, Moon J. A low-cure-temperature copper nano ink for highly conductive printed electrodes. Current Applied Physics 2009; (9): e157-e160. https://doi.org/10.1016/j.cap.2009.03.008

[10] Jang S, Seo Y, Choi J, Kim T, Cho J, Kim S, Kim D. Sintering of inkjet printed copper nanoparticles for flexible electronics. Scripta Materialia 2010; 62(5): 258-261. https://doi.org/10.1016/j.scriptamat.2009.11.011

[11] Kim YH, Kang YS, Lee WJ, Jo BG, Jeong JH. Synthesis of Cu Nanoparticles Prepared by Using Thermal Decomposition of Cu-oleate Complex. Molecular Crystals and Liquid Crystals 2006; 445(1): 231-238. https://doi.org/10.1080/15421400500366522

[12] Li W, Chen M. Synthesis of stable ultra-small Cu nanoparticles for direct writing flexible electronics. Applied Surface Science 2014; (290): 240-245. https://doi.org/10.1016/j.apsusc.2013.11.057

[13] Fouad OA, El-Shall MS. Microwave irradiation assisted growth of Cu, Ni, Co metals and/or oxides nanoclusters and their catalytic performance. Nano Brief Reports and Reviews 2012; 7(5): 1250034. https://doi.org/10.1142/s1793292012500348

[14] Joshi SS, Patil SF, Iyer V, Mahumuni S. Radiation induced synthesis and characterization of copper nanoparticles. Nanostructured Materials1998; 10(7): 1135-1144. https://doi.org/10.1016/S0965-9773(98)00153-6

[15] Solanki JN, Sengupta R, Murthy ZVP. Synthesis of copper sulphide and copper nanoparticles with microemulsion method. Solid State Sciences 2010; 12(9): 1560-1566. https://doi.org/10.1016/j.solidstatesciences.2010.06.021

[16] Panigrahi S, Kundu S, Ghosh S, Nath S, Pal T. General method of synthesis for metal nanoparticles. Nanoparticle Research 2004; 6(4): 411-414. https://doi.org/10.1007/s11051-004-6575-2

[17] Song, X, Sun, S, Zhang, W, Yin, Z. A method for the synthesis of spherical copper nanoparticles in the organic phase. Colloid and Interface Science 2004; 273(2): 463-469. https://doi.org/10.1016/j.jcis.2004.01.019

[18] Pileni MP, Gulik-Krzywicki T, Tanori J, Filankembo A, Dedieu JC. Template Design of Microreactors with Colloidal Assemblies: Control the Growth of Copper Metal Rods. Langmuir 1998; 14(26): 7359-7363. https://doi.org/10.1021/la980461m

[19] Kapoor S, Mukherjee T. Photochemical formation of copper nanoparticles in poly(N-vinylpyrrolidone). Chemical Physics Letters 2003; 370(1-2): 83-87. https://doi.org/10.1016/S0009-2614(03)00073-3

[20] Wu SH, Chen DH. Synthesis of high-concentration Cu nanoparticles in aqueous CTAB solutions. Colloid and Interface Science 2004; 273(1): 165-169. https://doi.org/10.1016/j.jcis.2004.01.071

[21] Ghosh Chaudhuri R, Paria S. Core/shell nanoparticles: Classes, properties, synthesis mechanisms, characterization, and applications. Chemical Reviews 2012; 112: 2373-2433. https://doi.org/10.1021/cr100449n

[22] Ilknur Tunç. Spectroscopic characterization and charging/discharging properties of bimetallic and coreshell Au-Ag nanoparticles, PhD thesis (2008), Department of Chemistry and the Institute of Engineering and Sciences of Bilkent University

[23] Magdassi S. The Chemistry of Inkjet Inks: World Scientific Publishing Co. Pte. Ltd 2010.

[24] Leff DV, Brandt L, Heath JR. Synthesis and Characterization of Hydrophobic, Organically-Soluble Gold Nanocrystals

Functionalized with Primary Amines. Langmuir 1996; 12(20): 4723-4730.
https://doi.org/10.1021/la960445u

[25] Khan A, Rahman K, Soo D, Hyun K. Direct printing of copper conductive micro-tracks by multi-nozzle electrohydrodynamic inkjet printing process. Materials Processing Technology 2012; 212(3): 700-706.
https://doi.org/10.1016/j.jmatprotec.2011.10.024

[26] Li W, Chen M. Synthesis of stable ultra-small Cu nanoparticles for direct writing flexible electronics. Applied Surface Science 2014. 290: 240-245.
https://doi.org/10.1016/j.apsusc.2013.11.057

[27] Nie X, Wang H, Zou J. Inkjet printing of silver citrate conductive ink on PET substrate. Applied Surface Science 2012; (261): 554-560.
https://doi.org/10.1016/j.apsusc.2012.08.054

[28] Shim I, Lee YII, Lee KJ, Joung J. An organometallic route to highly monodispersed silver nanoparticles and their application to ink-jet printing. Materials Chemistry and Physics 2008; 110(2-3); 316-321.
https://doi.org/10.1016/j.matchemphys.2008.02.020

[29] Huang Q, Shen W, Song W. Synthesis of colourless silver precursor ink for printing conductive patterns on silicon nitride substrates. Applied Surface Science 2012; 258(19): 7384-7388.
https://doi.org/10.1016/j.apsusc.2012.04.037

Received on 25-05-2017 Accepted on 03-06-2017 Published on 25-08-2017

DOI: https://doi.org/10.12974/2311-8792.2017.05.1